

**PRODUCER GAS CLEANING PROCESS FROM  
BIOMASS GASIFICATION AND ITS IMPACT ON  
SOLID OXIDE FUEL CELLS PERFORMANCE**

**ZIA UD DIN**

**UNIVERSITI SAINS MALAYSIA**

**2018**

**PRODUCER GAS CLEANING PROCESS FROM BIOMASS  
GASIFICATION AND ITS IMPACT ON SOLID OXIDE FUEL  
CELLS PERFORMANCE**

**by**

**ZIA UD DIN**

**Thesis submitted in fulfilment of the  
requirements for the degree of  
Doctor of Philosophy**

**May 2018**

## ACKNOWLEDGEMENT

Alhamdulillah Rabbil 'Alamin. Above all, I thank Allah for giving me the will and steadfastness to do this work specifically and cope with the life generally. The love and prayers of my parents are specially acknowledged for being the constant inspiration during this challenge.

I would like to express my deepest gratitude to my supervisor, Prof. Dr. Zainal Alimuddin Bin Zainal Alauddin for his invaluable and consistent support and guidance. It was a great opportunity to work under his supervision.

I would like to extend sincere thanks to Dr. Khaled Ali Al-Attab and other members of the biomass energy research group for all technical discussions and guidance in biomass laboratory. Also, acknowledged is the assistance of all the staff of School of Mechanical Engineering especially those of biomass laboratory and school's workshop.

I would like to acknowledge the Ministry of Higher Education Malaysia for financial support for PhD student at Universiti Sains Malaysia, Penang under USM Global Fellowship. USM Research University Individual (RUI) grant is also gratefully appreciated for financial support.

Special thanks to my beloved wife Mahwish Zia for her wordless and endless support and encouragement throughout this enduring process. Indebted thanks to her for taking care of our children Enaya Zia, Zaka Bin Zia and Radya Zia during the journey of my PhD. To our lovely children, thank you for understanding and prayers.

## TABLE OF CONTENTS

	<b>Page</b>
<b>ACKNOWLEDGEMENT</b>	ii
<b>TABLE OF CONTENTS</b>	iii
<b>LIST OF TABLES</b>	viii
<b>LIST OF FIGURES</b>	x
<b>LIST OF ABBREVIATIONS</b>	xvi
<b>LIST OF SYMBOLS</b>	xx
<b>ABSTRAK</b>	xxiii
<b>ABSTRACT</b>	xxv
<b>CHAPTER ONE: INTRODUCTION</b>	
1.1 Research background	1
1.2 Biomass integrated gasification–SOFC systems	3
1.3 Tar content and tar thermal cracking	6
1.4 Microwave heating	7
1.5 Problem statement	9
1.6 Objectives of the thesis	10
1.7 Scope of the thesis	10
1.8 Outline of the thesis	12
<b>CHAPTER TWO: LITERATURE REVIEW</b>	
2.1 Biomass materials	14
2.2 Biomass gasification	15
2.2.1 Downdraft gasifier	19
2.2.1(a) Gasifier performance	20
2.2.1(b) Effects of operating parameters on gasification process	21
2.2.2 Tar formation, composition and classification	22

2.2.2(a)	Tar definition	23
2.2.2(b)	Tar composition and classification	24
2.3	Tar thermal cracking	27
2.3.1	Thermal cracking mechanism	28
2.3.2	Effect of temperature and residence time on thermal cracking	30
2.3.3	Reaction kinetic model of tar thermal cracking	32
2.4	Microwave heating	35
2.5	Solid oxide fuel cells – working principle	39
2.5.1	SOFC designs	43
2.5.2	SOFC materials	44
2.5.3	Carbon deposition boundary prediction	46
2.6	Influence of PG contaminants on SOFC anodes and cleaning options	48
2.6.1	Particulates	48
2.6.2	Alkali metals	52
2.6.3	Tar	54
2.6.4	Sulfur compounds – mainly H <sub>2</sub> S	59
2.6.5	Halides – mainly HCl	64
2.6.6	Summary of tolerance limits and cleaning options for SOFC	67
2.7	Summary of Literature Review	70

### **CHAPTER THREE: EXPERIMENTAL METHODOLOGY**

3.1	Overall experimental flowchart and list of activities	72
3.2	Biomass gasification system	75
3.2.1	Biomass materials	75
3.2.2	Downdraft gasifier	76
3.2.3	Experimental procedure for gasifier characterization	76
3.3	Microwave tar cracking system	77
3.4	PG tar removal in MW tar cracking reactor	82
3.4.1	Producer gas tar removal	84
3.4.2	Conversion kinetics of tar thermal cracking	85
3.5	Design, fabrication and characterization of SOFC chamber	86
3.6	PG cooling system	89
3.7	PG cleaning system	92

3.7.1	PG compression system	92
3.7.2	H <sub>2</sub> S cleaning system	94
	3.7.2(a) Preparation of Impregnated-CSAC	95
	3.7.2(b) H <sub>2</sub> S adsorption column	96
3.7.3	Final quantification of PG and PG contaminants before SOFC	97
3.8	SOFC Experiments	98
3.8.1	SOFC testing equipment	98
3.8.2	Experimental procedure for SOFC testing	102
3.8.3	Prediction of carbon deposition on the SOFC anode	105
3.8.4	Post investigations of tested SOFC on PG	105
3.9	Characterization and analytical methods/ apparatus	105
3.9.1	Heating value of wood pellets	105
3.9.2	Proximate analysis	106
3.9.3	Ultimate analysis	107
3.9.4	PG sampling system	107
3.9.5	Tar and particulate analysis	109
3.9.6	Particulates/ash composition analysis	110
3.9.7	Analysis of PG	110
3.9.8	H <sub>2</sub> S and HCl analysis	111
3.9.9	Scanning electron microscopy (SEM)	112

## **CHAPTER FOUR: RESULTS AND DISCUSSIONS**

4.1	Biomass material characterization	113
4.2	Gasifier characterization	116
	4.2.1 Effect of gasification air flow rate	116
	4.2.2 Effect of equivalence ratio	117
	4.2.3 Temperature profiles	120
4.3	MW tar cracking reactor characterization	122
	4.3.1 Effect of MW power	122
	4.3.2 Effect of absorber material particle size	125
	4.3.3 Effect of gas flow rate – Determination of residence time	129
	4.3.4 SOFC chamber characterization	133
	4.3.5 Integration of gasifier with MW tar cracking reactor	135

4.4	Thermal cracking of PG tar in MW reactor	137
4.4.1	Dynamic temperature profile in MW reactor under temperature control	139
4.4.2	Tar and particulate conversion during thermal cracking	141
4.4.3	Comparison of thermal cracking of PG tar	145
4.4.4	Reaction kinetic model of PG tar	146
	4.4.4(a) Estimation of kinetic parameters	149
	4.4.4(b) Validation of kinetic model	150
	4.4.4(c) Removal efficiency estimation	151
4.5	Evaluation of the PG cooling system	154
4.6	Evaluation of the PG cleaning system	156
4.6.1	Particulates and Alkali compounds	156
4.6.2	Tar	159
	4.6.2(a) PG Compression as a tar removal method	159
	4.6.2(b) Tar condensation mechanism during PG compression	161
4.6.3	H <sub>2</sub> S – CSAC adsorber performance	166
4.6.4	HCl removal	167
4.6.5	Summary of PG cleaning results and cleaning chain configuration	168
4.7	SOFC performance on cleaned PG	170
4.7.1	Dynamic temperature profile in SOFC chamber under temperature control	171
4.7.2	Test campaign 1: 60 minutes operation on open circuit voltage	172
	4.7.2(a) OCV and characterization of starting/reducing anode	172
	4.7.2(b) Effect of temperature on cell performance	174
	4.7.2(c) Tendency of carbon deposition	178
	4.7.2(d) Voltage profile with time at OCV operation	181
4.7.3	Test campaign 2: 60 minutes operation under load – Test No. 3	184
4.7.4	Test campaign 3: 300 minutes operation under load – Test No. 4	191
4.7.5	Post investigations of tested SOFC on PG	194
4.7.6	Comparison of SOFC performance on PG with literature	196

<b>CHAPTER FIVE: CONCLUSIONS AND RECOMMENDATIONS</b>	
5.1 Conclusions	199
5.2 Recommendations for future work	202
<b>REFERENCES</b>	203
<b>APPENDICES</b>	
Appendix A – Evaluation of reaction kinetic model	
Appendix B – SOFC chamber drawings	
Appendix C – A planar SOFC I–V curve under H <sub>2</sub> provided by the supplier	
Appendix D – EXCEL calculations for gas compositions for SOFC testing	
<b>LIST OF PUBLICATIONS AND CONFERENCES</b>	



## LIST OF TABLES

	<b>Page</b>	
Table 2.1	Ultimate and proximate analysis of some biomass materials compared with bituminous coal (McKendry, 2002a; Zabaniotou, 2014)	15
Table 2.2	Overview of biomass gasification processes	16
Table 2.3	Overview of impurities in producer gas (Asadullah, 2014; Woolcock & Brown, 2013)	17
Table 2.4	Comparison of commonly used biomass gasifiers (Knoef, 2005; Ruiz et al., 2013)	19
Table 2.5	List of tar compounds from various gasifiers (Van Paasen et al., 2002)	25
Table 2.6	Description of tar classes developed by ECN (Van Paasen et al., 2004)	26
Table 2.7	Comparison of MW and conventional processing for thermo-chemical biomass conversion	36
Table 2.8	Dielectric loss tangent of some substances at a MW frequency of 2.45 GHz. Adapted from (Lidström et al., 2001; Menéndez et al., 2010; Yin, 2012)	39
Table 2.9	Properties of most commonly used SOFC components along with advantages and disadvantages adapted from (Jacobson, 2009)	45
Table 2.10	Main features of different particulate removal technologies	51
Table 2.11	Probable tolerance limits of contaminants for SOFC and their recommended cleaning options	68
Table 3.1	Some physical properties of wood pellets	76
Table 3.2	Technical specifications of the industrial MW oven	78
Table 3.3	Information of SiC products used in this research	80
Table 3.4	Specifications of the air compressor used for PG compression	92
Table 3.5	Specifications of the commercial coconut shell activated carbon (CSAC)	94
Table 3.6	Specifications of single SOFC used in this research work	98

Table 4.1	Characteristics of the used wood pellets	114
Table 4.2	Biomass gasification experimental runs	116
Table 4.3	Determination of effective reaction volume ( $V_R$ ), residence time ( $T_R$ ) and attained reaction temperatures inside the reactor based on different gas flow rates	132
Table 4.4	An average PG composition and main product distribution of sawdust wood pellets gasification in throatless downdraft gasifier	139
Table 4.5	Comparison of tar reduction efficiency and producer gas heating value under different treatment methods	147
Table 4.6	Kinetic parameters of tar conversion from PG in MW tar thermal cracking system	150
Table 4.7	Composition of residues with and without Carbon	157
Table 4.8	Tar component compounds in PG at the inlet of the compressor	162
Table 4.9	Summary of contaminants' cleaning results and their comparison with tolerance limits for SOFC	170
Table 4.10	Summary of tests conducted to evaluate the SOFC performance on cleaned PG	170
Table 4.11	OCV for the tested fuel feeds and their comparison with Nernst voltage	174
Table 4.12	Characteristics of the cleaned PG and SOFC along with the results for test No. 2	181
Table 4.13	Summary of characteristics of the cleaned PG and SOFC along with their results for test No. 3 (derived parameters are in italic)	190
Table 4.14	Comparison of SOFC performance on real PG in terms of measured voltage and cell degradation with other researchers in literature	198

## LIST OF FIGURES

	<b>Page</b>
Figure 1.1 Electrical efficiencies of SOFC compared with other energy conversion devices adapted from (Sharaf & Orhan, 2014)	2
Figure 1.2 Technical outline of a BIG–SOFC system	3
Figure 1.3 Conceptual illustration of heating gradient and temperature profile of a material in (a) conventional and (b) MW heating adapted from (Fernández et al., 2011)	8
Figure 2.1 Overview of impurities in biomass gasification gas (Nagel, 2008)	18
Figure 2.2 Sequential steps of gasification in throated (left) and throatless (right) fixed bed downdraft gasifier (Basu, 2010)	20
Figure 2.3 Formation and conversion of tar (Morf, 2001)	22
Figure 2.4 Tar evolution as a function of temperature (Milne et al., 1998)	23
Figure 2.5 Relationship between tar dew point and concentration of different tar classes 2-5 (Van Paasen et al., 2004)	27
Figure 2.6 Hydrogen shift mechanism during thermal treatment of tar compound (van der Hoeven, 2007)	29
Figure 2.7 Simplified reaction scheme of thermal conversion of aromatic hydrocarbons in the presence of hydrogen and steam (Jess, 1996)	34
Figure 2.8 Reaction scheme for thermal conversion of biomass gravimetric tar (Namioka et al., 2009)	34
Figure 2.9 Working principle of anode-supported internally reforming SOFC (Alfred, 2016)	40
Figure 2.10 Voltage losses and their dependency on current (Larminie & Dicks, 2003)	43
Figure 2.11 SOFC designs (a) planar on the left and tubular on the right (b) type of supports to SOFC adapted from (NTT, 2016)	44
Figure 2.12 (Left) proposed flow scheme for high temperature and (right) an experimentally tested intermediate temperature gas clean-up chain	70

Figure 3.1	List of overall experimental activities in this study (shown with chapter sub-headings)	73
Figure 3.2	Block diagram of overall experimental processes employed in this study	74
Figure 3.3	Schematic diagram of the biomass gasification system	75
Figure 3.4	Schematic drawing of the MW tar thermal cracking reactor	79
Figure 3.5	Industrial MW oven modified as the MW tar thermal cracking reactor	80
Figure 3.6	Schematic of the experimental setup of MW tar thermal cracking system	83
Figure 3.7	Experimental setup of the MW tar thermal cracking system	83
Figure 3.8	Temperature profile and reference temperature inside the reactor bed	85
Figure 3.9	SOFC chamber thermally integrated with the MW reactor	87
Figure 3.10	(a) SOFC chamber in two halves, (b) SOFC holder assembled inside SOFC chamber with the help of clamp	88
Figure 3.11	Schematic of the overall experimental set up showing all the system components	91
Figure 3.12	(a) Schematic diagram and (b) photograph of the carbonization unit	95
Figure 3.13	CSAC based H <sub>2</sub> S adsorption column	97
Figure 3.14	SOFC holder (a) front view showing the flow channels of both manifolds (b) side view of only one manifold, second is the same	99
Figure 3.15	(a) SOFC (b) Ag mesh (left), fibre glass seal (right)	100
Figure 3.16	SOFC assembly held by clamp (left), single SOFC setup details (right)	101
Figure 3.17	Procedural steps for SOFC 60 min/ 300 min duration operations (simultaneous gasifier operation corresponding to time shown inside the figure)	103
Figure 3.18	Schematic of the apparatus used in PG sampling system	108
Figure 4.1	Effect of gasification air flow rate and corresponding PG production rate and biomass consumption rate	117

Figure 4.2	Effect of equivalence ratio and air flow rate on PG composition and LHV	119
Figure 4.3	Effect of equivalence ratio on the oxidation zone temperature	120
Figure 4.4	Average gasifier outlet temperature at various PG flow rates	121
Figure 4.5	Temperature evolution inside the reactor under different MW powers (absorber material; 8 mm $\phi$ SiC balls, bed height; 500 mm, gas flow rate; 120 LPM)	123
Figure 4.6	Absorption power efficiency under different MW powers (absorber material; 8 mm $\phi$ SiC balls, bed height; 500 mm, gas flow rate; 120 LPM)	125
Figure 4.7	Temperature evolution inside the reactor with different particle sizes of absorber material (MW power; 2.4 kW, bed height; 500 mm, gas flow rate; 120 LPM)	126
Figure 4.8	Absorption power efficiency with different particle sizes of absorber material (MW power; 2.4 kW, bed height; 500 mm, gas flow rate; 120 LPM)	127
Figure 4.9	Pressure drop inside the reactor bed with different sizes of absorber material at 1250 $^{\circ}$ C (MW power; 2.4 kW, gas flow rate; 120 LPM, bed height; 500 mm)	128
Figure 4.10	Temperature evolution inside the reactor under different gas flow rates (absorber material; 8 mm $\phi$ SiC balls, MW power; 2.4 kW, bed height; 500 mm)	129
Figure 4.11	Longitudinal temperature profiles inside the MW reactor under different gas flow rates (absorber material; 8 mm $\phi$ SiC balls, MW power; 2.4 kW)	131
Figure 4.12	Absorption power efficiency under different gas flow rates (absorber material; 8 mm $\phi$ SiC balls, MW power; 2.4 kW)	132
Figure 4.13	Possible attainable temperatures inside SOFC chamber with respect to the temperature evolution inside MW reactor under different gas flow rates (MW reactor with absorber bed material; 8 mm $\phi$ SiC balls, MW power; 2.4 kW)	134
Figure 4.14	Gasifier–MW tar cracking reactor flow diagram	135
Figure 4.15	Temperature profile evolution with the running time of gasifier operation at ER of 0.33 and PG production rate of 263 LPM	137
Figure 4.16	PG composition and LHV profiles with the running time of gasifier operation on sawdust wood pellets at the ER of 0.33	138

Figure 4.17	A typical temperature profile inside MW reactor and duty cycle of magnetron for the target thermal cracking temperature of 1250 °C	140
Figure 4.18	Conversion of PG tar as a function of reaction temperatures at constant residence time of 0.7 s	142
Figure 4.19	Conversion of PG particulates as a function of reaction temperatures at constant residence time of 0.7 s	143
Figure 4.20	PG composition and LHV at various thermal cracking temperatures	144
Figure 4.21	Arrhenius plot for the calculations of activation energy and pre-exponential factor for thermal cracking of PG tar	149
Figure 4.22	Predicted conversion efficiencies against experimental conversion efficiencies from thermal cracking of PG tar	151
Figure 4.23	Predicted model (line) in comparison with the experimental data (circle symbol) of conversion efficiencies from thermal cracking of PG tar	152
Figure 4.24	Estimated PG tar conversion by thermal cracking against the residence time at 900 °C (re-calculated at the fixed pre-exponential factor of $3.16 \times 10^{15} \text{ s}^{-1}$ )	154
Figure 4.25	Temperature profile of the cooling system	155
Figure 4.26	Quantification of particulates in the cleaning chain	158
Figure 4.27	Tar reduction via PG compression at 0.8 and 0.2 MPa <sub>g</sub>	159
Figure 4.28	PG flare visualization (a) before compression (tar = 138 mg Nm <sup>-3</sup> ) (b) after compression (tar = 24 mg Nm <sup>-3</sup> )	161
Figure 4.29	Proposed tar condensation mechanism via compression of producer gas (DP = dew point, PDP = pressure dew point, PG = producer gas, T <sub>amb</sub> = ambient temperature, T <sub>comRT</sub> = temperature of PG in compressor receiver tank)	165
Figure 4.30	Quantification of tar in the cleaning chain	166
Figure 4.31	H <sub>2</sub> S removal in CSAC fixed bed adsorber (temperature; ambient (35 °C), residence time; 15.1 s)	167
Figure 4.32	PG cleaning chain at mixed high and low temperatures employed in this study	169
Figure 4.33	A typical temperature profile inside SOFC chamber and duty cycle of magnetron for the target SOFC operation temperature of 800 °C	171

Figure 4.34	OCV of the cell during reduction of anode at different H <sub>2</sub> concentrations and 3% H <sub>2</sub> O balance N <sub>2</sub>	173
Figure 4.35	C–H–O ternary diagram showing the carbon deposition region on the left side of thermodynamic equilibrium prediction lines of 800 °C, 700 °C, 600 °C under OCV	176
Figure 4.36	I–V curves taken at the 5 <sup>th</sup> minute after shifting the fuel to clean PG (with 10%H <sub>2</sub> O) at different temperatures	178
Figure 4.37	I–V curves taken on clean PG (with 10%H <sub>2</sub> O) at the start (symbol) and after 1 h operation on PG (dashed line) at open circuit at different temperatures	179
Figure 4.38	(a) Composition of PG (with 10% H <sub>2</sub> O) over the SOFC operation time (b) PG LHV and corresponding OCV vs time during the SOFC operation at 800 °C	182
Figure 4.39	OCV and Nernst voltage and their difference during operation on PG (with 10%H <sub>2</sub> O) at 800 °C	184
Figure 4.40	(a) Composition of PG (with 10% H <sub>2</sub> O) and corresponding LHV (b) comparison of Nernst voltage and cell voltage over time during all test phases at 800 °C (a = operation on H <sub>2</sub> /N <sub>2</sub> , b = operation on PG at OCV and c = operation on PG at 260 mA cm <sup>-2</sup> )	185
Figure 4.41	Cell voltage, power density, corresponding LHV of PG and fuel utilization vs time (b = operation on PG at OCV and c = operation on PG at 260 mA cm <sup>-2</sup> ) at 800 °C	187
Figure 4.42	LHV and corresponding S/C ratio of anode feed gas (PG with 10 vol% H <sub>2</sub> O) vs time during SOFC operation on PG for Test No. 3	188
Figure 4.43	I–V curves taken on 45/55 vol% H <sub>2</sub> /N <sub>2</sub> (with 3%H <sub>2</sub> O) before (symbol) and after 60 min operation on PG under constant current density of 260 mA cm <sup>-2</sup> (dashed line)	189
Figure 4.44	LHV of PG (with 10% H <sub>2</sub> O) fed to SOFC and obtained cell voltage, fuel utilization and power density over time during Tests No. 3 & 4. (a = operation on H <sub>2</sub> /N <sub>2</sub> , b = operation on PG at OCV and c = operation on PG at 260 mA cm <sup>-2</sup> )	192
Figure 4.45	I–V curves taken on 45/55 vol% H <sub>2</sub> /N <sub>2</sub> (with 3%H <sub>2</sub> O) before (symbol) and after operation on PG under constant current density of 260 mA cm <sup>-2</sup> (dashed line)	193
Figure 4.46	C–H–O ternary diagram showing the carbon deposition region on the left side of thermodynamic equilibrium prediction line of 800 °C and plotted points corresponding to PG composition	

given in Table 4.12 fed to SOFC at OCV and under load conditions

194

Figure 4.47 SEM images of anode surface (a) of an original cell (b) after the operation on PG for 300 min under current density of  $260 \text{ mA cm}^{-2}$  in this study (c) detailed image of the same cell as shown in (b) ( $\times 10,000$  magnification). (d) The SEM image of Ni/YSZ anode showing carbon deposition taken from (Hua et al., 2014) and presented here only for the comparison purpose between the cell without carbon deposition from this study and carbon deposited anode from literature (Hua et al., 2014)

195



## LIST OF ABBREVIATIONS

AC	Activated carbon
Al <sub>2</sub> O <sub>3</sub>	Alumina
Ag	Silver
Ar	Argon
C	Carbon
Ca	Calcium
CaO	Calcium Oxide (Calcite)
Ce	Cerium
CeO <sub>2</sub>	Ceria
CD	Current Density
CH <sub>4</sub>	Methane
CHP	Combined Heat and Power
CO	Carbon Monoxide
CO <sub>2</sub>	Carbon Dioxide
C <sub>n</sub> H <sub>m</sub>	Representing Hydrocarbons Lower Than Tar Compounds
C <sub>x</sub> H <sub>y</sub>	Representing Tar Compounds
CPG	Compressed Producer Gas
CSAC	Coconut Shell Activated Carbon
EDS	Energy Dispersive Spectroscopy
EIA	Energy Information Administration
ER	Equivalence Ratio
ESP	Electrostatic Precipitator
FAD	Free Air Delivery

FC	Fixed Carbon
FCC	Fluid Catalytic Cracking
FEPA	Federation of European Producers of Abrasives
FICFB	Fast Internally Circulating Fluidized-bed Gasifier
FU	Fuel Utilization
GC	Gas Chromatography
H <sub>2</sub>	Hydrogen
H <sub>2</sub> O	Water or Steam
HPG	Hot Producer Gas
H <sub>2</sub> S	Hydrogen Sulfide
HCl	Hydrogen Chloride
He	Helium
HHV <sub>b</sub>	Higher Heating Value of Biomass (MJ kg <sup>-1</sup> )
HHV <sub>PG</sub>	Higher Heating Value of Producer Gas (MJ Nm <sup>-3</sup> )
ICE	Internal Combustion Engines
I-V (curves)	Current Voltage (curves)
IGCC	Integrated Biomass Gasification and Combined Cycle
K	Potassium
LAH	Light Aromatic Hydrocarbon
LHV	Lower Heating Value (MJ Nm <sup>-3</sup> )
LHV <sub>b</sub>	Lower Heating Value of Biomass (MJ kg <sup>-1</sup> )
LHV <sub>PG</sub>	Lower Heating Value of Producer Gas (MJ Nm <sup>-3</sup> )
Li	Lithium
LPAH	Light Poly-Aromatic Hydrocarbon
LPG	Liquefied Petroleum Gas

LPM	Litres per Minute
Mg	Magnesium
MgO	Magnesium Oxide (Magnesite)
MS	Mass Spectrophotometry
MW	Microwave
N <sub>2</sub>	Nitrogen
Na	Sodium
NH <sub>3</sub>	Ammonia
NO <sub>x</sub>	Nitrogen Oxide
Ni	Nickel
NiO	Nickel Oxide
Ni/YSZ	Nickel Yttria Stabilized Zirconia
NTT	Nippon Telegraph and Telephone (Japan)
O <sub>2</sub>	Oxygen
OCV	Open Circuit Voltage
PAH	Poly-Aromatic Hydrocarbon
PEM	Polymer Electrolyte Membrane
PG	Producer Gas
PID	Proportional band, Integral and Derivative Time Action
ppm <sub>w</sub>	parts per million by weight
Pt	Platinum
SEE	Standard Error of the Estimate
SEM	Scanning Electron Microscopy
SiC	Silicon Carbide
SiO <sub>2</sub>	Silica

SO <sub>2</sub>	Sulfur Dioxide
SOFC	Solid Oxide Fuel Cells
SS	Stainless Steel
TCD	Thermal Conductivity Detector
VOC	Volatile Organic Compound
VM	Volatile Matter
WGS	Water Gas Shift
ZrO <sub>2</sub>	Zirconia

## LIST OF SYMBOLS

$C_{Tin}$	Inlet tar concentration ( $\text{g Nm}^{-3}$ )
$C_{Tout}$	Outlet tar concentration ( $\text{g Nm}^{-3}$ )
$C_T$	Tar concentration ( $\text{g Nm}^{-3}$ )
$D_p$	Penetration depth of microwave power (m)
$E$	Activation energy ( $\text{kJ mol}^{-1}$ )
$E_{rms}$	Electric field ( $\text{V m}^{-1}$ )
$f$	Frequency (Hz)
$F$	Faraday constant (96485 Coulombs)
$F_T$	Mass of the remaining condensed tar (g)
$F_{T,0}$	Initial mass of tar (g)
$\Delta G$	Gibbs free energy
$k$	Kinetic rate constant ( $\text{s}^{-1}$ )
$k_0$	Pre-exponential/frequency factor ( $\text{s}^{-1}$ ) or ( $\text{m}^3 \text{kg}^{-1} \text{h}^{-1}$ )
$K_{(T)}$	Equilibrium constant of a reaction
$K_{MD}$	Equilibrium constant of methane decomposition reaction
$K_{STR}$	Equilibrium constant of steam reforming reaction
$K_{WGS}$	Equilibrium constant of water gas shift reaction
$\dot{m}_b$	Mass flow rate of the biomass fuel ( $\text{kg h}^{-1}$ )
$\dot{n}_f$	Anode molar flow ( $\text{mol min}^{-1}$ )
$\dot{n}_c$	Cathode molar flow ( $\text{mol min}^{-1}$ )
$P_{abs}$	Absorbed microwave power (W)
$P_{MW}$	Output power of the microwave oven (W)

$P_o$	Incident microwave power at the material surface (W)
$P(z)$	Microwave power at distance $z$ (W)
$p_i$	Partial pressure
$Q$	Gas flow rate ( $\text{m}^3 \text{h}^{-1}$ )
$Q_{\text{cond}}$	Heat conduction (W)
$Q_{\text{conv}}$	Heat convection (W)
$Q_{PG}$	Volumetric flow rate of the producer gas ( $\text{Nm}^3 \text{h}^{-1}$ )
$Q_{\text{rad}}$	Heat radiation (W)
$\dot{Q}_f$	Fuel flow rate at anode ( $\text{ml min}^{-1}$ )
$\dot{Q}_c$	Air flow rate at cathode ( $\text{ml min}^{-1}$ )
$r_T$	Conversion rate of tar ( $\text{g Nm}^{-3} \text{s}^{-1}$ ) or ( $\text{g s}^{-1}$ )
$R$	Universal gas constant ( $0.008314 \text{ kJ mol}^{-1} \text{ K}^{-1}$ )
$S/C$	Steam to carbon ratio
$t$	Time period (s)
$\tan \delta$	Loss tangent
$T$	Reaction temperature (K)
$T_{\text{ambient}}$	Ambient or surrounding temperature (K)
$T_{\text{inlet}}$	Reactor inlet temperature (K)
$T_R$	Residence time (s) or ( $\text{kg h m}^{-3}$ )
$\bar{T}$	Average temperature within the reactor (K)
$U$	Overall heat transfer coefficient ( $\text{W m}^{-2} \text{K}^{-1}$ )
$U_f$	Fuel utilization factor
$U_{O_2}$	Oxygen utilization factor
$V$	Volume of absorber material ( $\text{m}^3$ )
$V_{\text{cell}}$	SOFC voltage (V)

$V_R$	Effective reaction volume with respect to empty reactor volume ( $\text{m}^3$ )
$x_{CH_4}$	Volume fraction of methane
$x_{CO}$	Volume fraction of carbon monoxide
$x_{H_2}$	Volume fraction of hydrogen
$X_T$	Tar conversion
$\varepsilon$	Emissivity of material
$\varepsilon'$	Dielectric constant
$\varepsilon''$	Dielectric loss factor
$\varepsilon^*$	Complex dielectric constant
$\varepsilon_0$	Permittivity of free space ( $8.85 \times 10^{-12} \text{ F m}^{-1}$ )
$\rho$	Density ( $\text{kg m}^{-3}$ )
$\sigma$	Stefan-Boltzman constant ( $5.67 \times 10^{-8} \text{ W m}^{-2} \text{ K}^{-4}$ )
$\eta_P$	Absorption power efficiency (%)
$\lambda_0$	Free space wavelength of the microwave radiation (12.23 cm)
$\phi$	Thiele modulus
$\emptyset$	Diameter (m)

**PROSES PEMBERSIHAN GAS PENGELUAR DARI GASIFIKASI BIOJISIM  
DAN KESANNYA TERHADAP PRESTASI SEL BAHAN API OKSIDA  
PEPEJAL (SOFC)**

**ABSTRAK**

Gas pengeluar (PG) yang diperolehi daripada biojisim boleh ditukarkan kepada tenaga elektrik secara cekap di dalam sel bahan api oksida pepejal (SOFC) pada suhu operasi antara 700–900°C jika bahan-bahan tercemar dibersihkan secukupnya daripada PG terutamanya tar. Antara pilihan kaedah untuk pembersihan tar, haba peretak menawarkan kelebihan dalam peningkatan nilai pemanasan PG dengan meretakkan tar kepada gas yang berguna dan haba yang diperolehi boleh digunakan sebagai sumber haba kepada SOFC yang mana ianya merupakan proses yang ekonomik untuk sistem berskala besar. Walaubagaimanapun, sistem haba peretak tar sedia ada adalah berskala makmal dan berdasarkan pada relau elektrik yang kurang cekap dan kos yang mahal. Sebagai alternatif, sistem haba peretak menggunakan pemanasan microwave (MW) adalah lebih cekap dan menguntungkan serta mempunyai potensi untuk proses berskala besar. Dalam kajian ini, Ketuhar MW industri yang diubahsuai telah dibangunkan dan dicirikan untuk haba peretak tar dan digabungkan dengan pengegas aliran bawah 10 kW<sub>th</sub>. Haba deria PG dari reaktor peretak tar MW telah dikekalkan didalam bekas keluli tahan karat (SS) untuk 60 W operasi SOFC tunggal. Kemudian PG melalui proses penyejukan sebelum dimampatkan di dalam pemampat sebagai mekanisma pembersihan tar daripada biojisim yang selanjutnya. Bendasing dan sisa-sisa logam alkali dan HCl disingkirkan melalui proses penyejukan dan penapisan. Baki bahan pencemar H<sub>2</sub>S pula disingkirkan menggunakan karbon teraktif daripada tempurung kelapa yang



telah direndam dalam urea (CSAC) sebelum PG termampat yang telah bersih disalurkan ke SOFC di dalam bekas SS haba bersepadu. Hasil eksperimen menunjukkan bahawa MW yang menggunakan tenaga yang rendah bagi reaktor peretak tar telah menukarkan 95% bendasing dan 93% tar kepada gas mudah bakar menghasilkan nilai pemasangan tertinggi iaitu sebanyak  $5.53 \text{ MJ Nm}^{-3}$  pada suhu  $1250 \text{ }^\circ\text{C}$ . Tar telah dikurangkan daripada  $1703 \text{ mg Nm}^{-3}$  kepada  $140 \text{ mg Nm}^{-3}$ . Kajian kinetik mendedahkan kadar penukaran tar adalah 1.7 kali lebih cepat dengan pemanasan MW berbanding pemanasan konvensional. Suhu PG yang tinggi ketika keluar dari reaktor MW melebihi  $800 \text{ }^\circ\text{C}$  adalah sesuai untuk operasi SOFC oleh itu penggunaan relau elektrik tidak diperlukan. Pemampatan PG di dalam pemampat terus dapat mengurangkan tar kepada  $22 \text{ mg Nm}^{-3}$  menghasilkan 84% kecekapan penyingkiran. Semua bendasing PG telah berjaya dikurangkan lebih rendah daripada had toleransi SOFC menggunakan sistem pembersihan yang telah dicipta. SOFC menghasilkan voltan yang stabil sebanyak  $0.865 \text{ V}$  sepanjang tempoh ujikaji dengan ketumpatan arus iaitu  $260 \text{ mA cm}^{-2}$  tanpa menunjukkan sebarang degradasi yang ketara di bawah operasi PG dengan nisbah S/C = 0.3 yang rendah tetapi masih bebas pendedapan karbon termodinamik. Satu unit SOFC mampu menghantar  $23 \text{ W}$  kuasa dengan kecekapan elektrik sebanyak 24% pada faktor penggunaan bahan api yang rendah iaitu 36. PG sebagai bahan bakar tidak menyebabkan sebarang kesan kemerosotan pada struktur mikro anod. Prestasi SOFC di bawah profil haba yang berterusan oleh PG berhaba panas adalah setara dengan sel-sel yang beroperasi menggunakan relau elektrik dengan pengawal suhu dalam masa yang sama.

**PRODUCER GAS CLEANING PROCESS FROM BIOMASS  
GASIFICATION AND ITS IMPACT ON SOLID OXIDE FUEL CELLS  
PERFORMANCE**

**ABSTRACT**

Biomass derived producer gas (PG) can be efficiently converted into electricity in solid oxide fuel cells (SOFC) at their operating temperature between 700–900 °C if sufficiently cleaned from PG contaminants especially tar. Amongst the tar cleaning options, thermal cracking offers the advantage of increasing the PG heating value by cracking tar into useful gases and the heat available can be utilized as heat source for SOFC operation. However, current tar thermal cracking systems are at lab-scale and are based on less efficient and expensive electric furnaces. Alternatively, thermal cracking system based on Microwave (MW) heating is rather more efficient and cost effective and has the potential for process scale-up. In this work, a modified industrial MW oven was developed and characterized for tar thermal cracking and integrated with a 10 kW<sub>th</sub> downdraft gasifier. The sensible heat of PG from MW tar cracking reactor was preserved in a stainless steel (SS) chamber for the operation of a 60 W single SOFC. PG was then subjected to a cooling process prior to compression in a compressor as a further tar cleaning mechanism of biomass tar. Particulates and traces of alkali metals and HCl were removed via cooling and filtration processes. The remaining contaminant H<sub>2</sub>S was removed using urea impregnated coconut shell activated carbon (CSAC) before feeding the cleaned compressed PG to a SOFC in a thermally insulated stainless steel chamber. The experimental work showed that MW tar cracking reactor converted 95% of

particulates and 93% of tar into combustible gases resulting in the highest heating value of 5.53 MJ Nm<sup>-3</sup> at 1250 °C. Tar was reduced from 1703 mg Nm<sup>-3</sup> to 140 mg Nm<sup>-3</sup>. Kinetic studies revealed that tar conversion rate was 1.7 times faster under MW heating as compared to conventional heating. The high temperature PG exiting MW reactor of above 800 °C is suitable for SOFC operation thus omitting an electric furnace otherwise required to maintain SOFC operating temperature. The compression of PG in a compressor further reduced tar to 22 mg Nm<sup>-3</sup> exhibiting 84% removal efficiency. All PG contaminants were successfully reduced below the probable tolerance limits for SOFC using the designed cleaning system. SOFC exhibited the stable voltage of 0.865 V for the tested duration of 300 min under current density of 260 mA cm<sup>-2</sup> without showing any significant degradation under PG operation with low S/C=0.3 but still under thermodynamic carbon deposition free conditions. A single SOFC delivered the power of 23 W with the electrical efficiency of 24% at the low fuel utilization factor of 36%. PG as fuel did not cause any deteriorating effects on anode microstructure. The SOFC exhibited comparable performance under thermal profile sustained by hot PG with those of the cells operated in temperature controlled electric furnaces in similar conditions.

## **CHAPTER ONE**

### **INTRODUCTION**

#### **1.1 Research background**

The global energy consumption is primarily covered by fossil fuels and will continue to produce approximately 75% of the world's primary energy by 2040 (EIA, 2017). At the same time, world emission of carbon dioxide has increased by 44% above 1993 levels by 2015 making the earth likely to warm by 1.7–4.9 °C from the period 1990–2100 (Nejat et al., 2015). Such an energy scenario may lead to disastrous outcomes if alternative fuels and alternate energy systems are not developed and utilized. Among the alternative options, biomass and fuel cells have recently received significant attention.

Biomass is considered a renewable energy source if it is based on sustainable utilization. Also, the residues and wastes as biomass feedstock are part of the short carbon cycle, their use for energy purposes has a minimal extra greenhouse gas emissions. Its energy potential is promising due to its evenly dispersed source and availability worldwide. Bioenergy based on biomass and waste would sustainably contribute between a quarter and a third of global primary energy supply in 2050 (IEA, 2016).

Fuel cell is an electrochemical device that converts the chemical energy of the fuel directly into electrical energy (without combustion) cleanly and efficiently and produces water mainly as its by-product. While low temperature fuel cells operate mainly with hydrogen as fuel, for high temperature SOFCs, hydrogen,

carbon monoxide, methane and their mixtures are considered as good fuel. The high operating temperature of SOFCs produces high quality heat by-product which can be used for co-generation or for use in combined cycle applications. They are more efficient in converting energy to electricity than internal combustion engines and most combustion systems as shown in Figure 1.1.

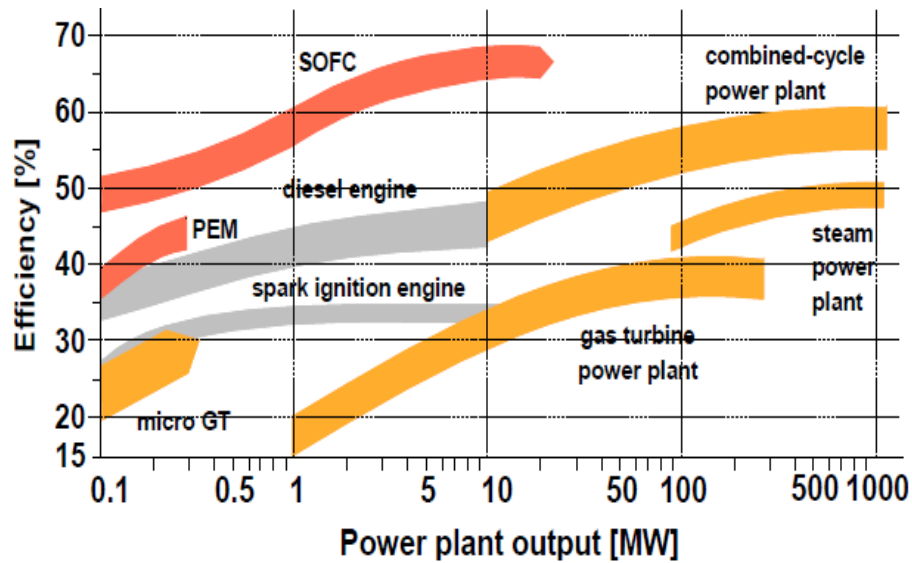


Figure 1.1: Electrical efficiencies of SOFC compared with other energy conversion devices adapted from (Sharaf & Orhan, 2014)

Traditionally fossil fuels are mainly converted into electricity and the world net electricity generation is expected to increase by 93 % in 2040 (EIA, 2017). Thus, the increased demand of electricity consumption requires increasing the efficiency of the electricity production. Among the biomass conversion pathways, the gasification of biomass in a gasifier allows the application of more efficient energy conversion cycles as compared to biomass combustion systems. A promising approach to achieve higher efficiencies is the use of SOFCs with biomass gasification referred to as “Biomass Integrated Gasification–SOFC (BIG–SOFC) systems”. Such systems are expected to show higher efficiencies even at a few hundred kW levels as

compared to their competing systems such as gasification–ICE and gasification–turbine systems. Modelling studies have shown that efficiencies can be enhanced significantly to 60–70%, if the high quality exhaust heat from SOFC is used in gas turbines downstream (Aravind et al., 2009).

## 1.2 Biomass integrated gasification–SOFC systems

Outline of the core components of BIG–SOFC systems is given in Figure 1.2. The first step in this technology is converting the biomass into a combustible mixture of gases referred to as producer gas (PG) through the process of gasification inside a gasifier. The PG consists of hydrogen, carbon monoxide, carbon dioxide, methane, nitrogen, water vapour and additionally some contaminants. The contaminants present in PG from biomass gasification include tar, particulates and traces of alkali metals, sulfur compounds mainly  $H_2S$  and halides mainly  $HCl$ . These contaminants are harmful and are required to be sufficiently removed in the second step. After cleaning, PG is compressed so that it could be fed to SOFC for electricity (and heat) generation in the last step of this technology.

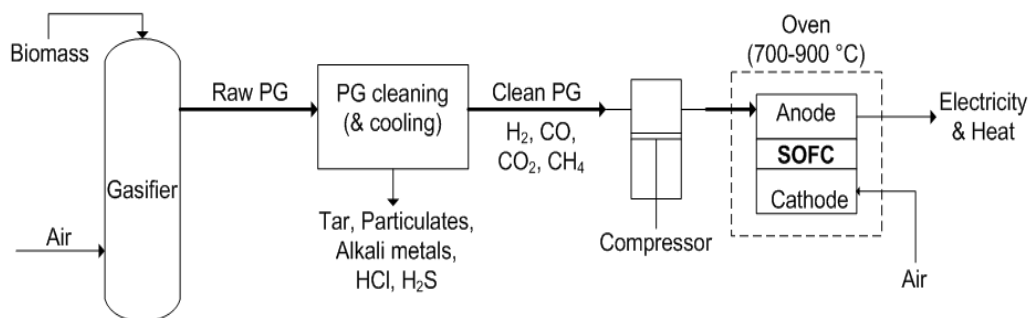


Figure 1.2: Technical outline of a BIG–SOFC system

In SOFC, the fuel is fed to the anode side (Figure 1.2) which electrochemically converts  $H_2$  and CO present in the PG into electricity while  $CH_4$  is internally reformed into  $H_2$  and CO. This is due to the reason that SOFC operates at high temperatures (700–900 °C) and contains nickel catalyst in their anode. SOFC are characterised by their high operating temperature which is conventionally maintained by an electric furnace which is an energy intensive requirement. Especially when it comes to large systems this would be a huge energy input requirement.

Amongst the contaminants, tar is the most notorious and generated in the highest quantities from the gasifier followed by particulates. Tar can induce carbon deposition on the nickel of SOFC anode, deactivating the catalyst resulting in degradation of SOFC (Papurello et al., 2016). Although alkali metals, HCl and  $H_2S$  are present in PG at the trace levels in the amounts of ppm, their removal is essential because even a few ppm of their presence could be detrimental to SOFC. They are adsorbed on the nickel anode, covering the active sites, inhibiting the fuel adsorption leading to the reduction of fuel oxidation and cell performance referred to as the poisoning of SOFC anodes (Błesznowski et al., 2013; Boldrin et al., 2015). Generally, a chain of gas cleaning units has to be applied to remove the contaminants from PG to meet their tolerance limits for SOFC (Aravind et al., 2013). Alkali metals and HCl (after condensation into particles) together with particulates could be removed from PG all together using experienced and mature technologies such as cyclones, scrubbers and other particulate filtration devices at low (near ambient) temperatures. The biggest problem at such low temperatures involves tar condensation resulting in clogging and fouling of the equipment. Hence, tar removal is highly recommended near the gasification temperatures.

Keeping in view the above mentioned two major requirements for BIG–SOFC systems i.e. (i) energy input to maintain SOFC operating temperature of 700–900 °C and (ii) removal of tar near gasification temperatures, a novel technique should be adopted which could address both the requirements simultaneously.

Most of the work done so far on SOFC operation used simulated PG which has compositions similar to real PG. These performances show that if PG is sufficiently cleaned, it will not exhibit challenging problems for SOFC (Aravind et al., 2005; Le Gal La Salle et al., 2017; Lebreton et al., 2015). There are only a few examples till date in which SOFCs have been coupled with real biomass gasifiers. One kW SOFC stack was operated on PG avoiding carbon deposition satisfactorily but catalytic partial oxidation was employed between the updraft gasifier and SOFC (Nagel et al., 2011). As part of the EU Framework 6 “BioCellus” project (Frank et al., 2008), single planar SOFCs (enclosed in electric furnaces at 850 °C) were operated with three different gasifiers in Europe. A cell operated successfully on PG with tar load of 3 g Nm<sup>-3</sup> from an autothermal fixed bed downdraft gasifier for less than 2 h but with steam to carbon ratio (S/C) of 3.4 (Hofmann et al., 2008). Similar cell showed stable performance for about 1 h on tar laden PG up to 10 g Nm<sup>-3</sup> from circulating fluidized bed gasifier but again with S/C of 5.1 (Hofmann et al., 2009). In a promising test, similar cell showed stable performance with negligible degradation for 150 h on PG from a two stage Viking gasifier with moderate S/C of 0.5 (Hofmann et al., 2007). But the PG was tar free in this case because of the separation of pyrolysis from gasification in the two stage gasifier. The particulates, H<sub>2</sub>S and HCl were removed from PG before feeding it to SOFC in all the three cases. It is noted that SOFC investigations on PG with considerable tar load are done for short running times (1–2 h) and in steam–rich conditions which help inhibit carbon



deposition but leads to low electrical (SOFC) efficiency. Therefore, coupling of real biomass gasifiers and utilization of PG in SOFCs at low S/C ratios has not yet been fully investigated. This challenging approach of operating SOFC without the addition of excessive steam will require the removal of tar from PG. The same is also required to avoid the clogging and fouling of the equipment.

### **1.3 Tar content and tar thermal cracking**

Tar is complex mixture of diverse organic (aromatic) compounds formed during pyrolysis and successive reactions with char. The tar yield from biomass gasification varies between 0.5 and 150 g Nm<sup>-3</sup> depending upon the types of gasifiers, feedstock used and operating conditions, while the recommended tar tolerance limits for compressors, internal combustion engines and gas turbines are 500 mg Nm<sup>-3</sup>, 100 mg Nm<sup>-3</sup> and 5 mg Nm<sup>-3</sup> respectively (Milne et al., 1998). The tar tolerance limits for SOFC are not agreed upon yet in literature however tar has been recognized as a major problem for SOFCs (Pumiglia et al., 2017).

Generally, high temperature tar removal methods include catalytic and thermal cracking of tar. However, most of the catalysts used in catalytic tar cracking are prone to deactivation due to (i) poisoning mostly sulfur poisoning, (ii) fouling, (iii) thermal degradation, (iv) erosion (v) attrition and (vi) phase transformation putting limits to scale up of systems.

Thermal cracking decomposes tar at temperatures from 1000–1300 °C with residence time between 1–12 s (Jess, 1996; Zhang et al., 2010). Higher temperatures need shorter residence times. It was demonstrated that naphthalene removal efficiency was 80% at 1075 °C with residence time of 5 s while it takes 1 s at 1150°C (Fjellerup et al., 2005). In another study it was shown that 0.5 s is enough for

sufficient tar cleaning at 1250 °C with 19% increase in the energy content of the gas (Brandt & Henriksen, 2000). Tar thermal cracking seems advantageous because it increases the heating value of the gas and has the potential of uninterrupted process with the possibility for process scale up. Certainly, the high reaction temperatures require high energy input making it uneconomical. Anis et al. have recently studied thermal tar cracking (at 1200 °C) using low energy intensive microwave (MW) and found that PG quality was upgraded significantly with increase in CO and H<sub>2</sub> content with tar removal efficiency of 90% (Anis & Zainal, 2013). If tar cracking using low energy intensive MW could be scaled up for commercial gasifiers, this development will be significant towards successful use of biomass gasification technologies in general and for BIG–SOFC systems in particular because the heat generated for tar cracking could be used for operating SOFC hence eliminating additional heat source (electric furnace).

#### **1.4 Microwave heating**

In conventional heating, the heat is transferred to the material from an external heat source by the mechanisms of convection, conduction and radiation. Heat is then transferred from the surface towards the centre of the material by thermal conduction. Heating process in MW technology is the reverse of conventional heating. Microwaves can penetrate the materials and deposit energy within them which results in “volumetric” heating in which heat can be generated throughout the volume of the material (Kostas et al., 2017). The temperature of the material becomes higher than the surroundings which is opposite in conventional heating in which the furnace cavity has to reach the operating temperature first to begin heating the material. These different mechanisms of heating cause opposite

temperature distribution and thermal gradient as depicted in Figure 1.3. As a result of this unique inverse and “volumetric” heating mechanism in MW, energy transfer efficiency increases and process heating time reduces because of the reason that heating effect is almost instantaneous.

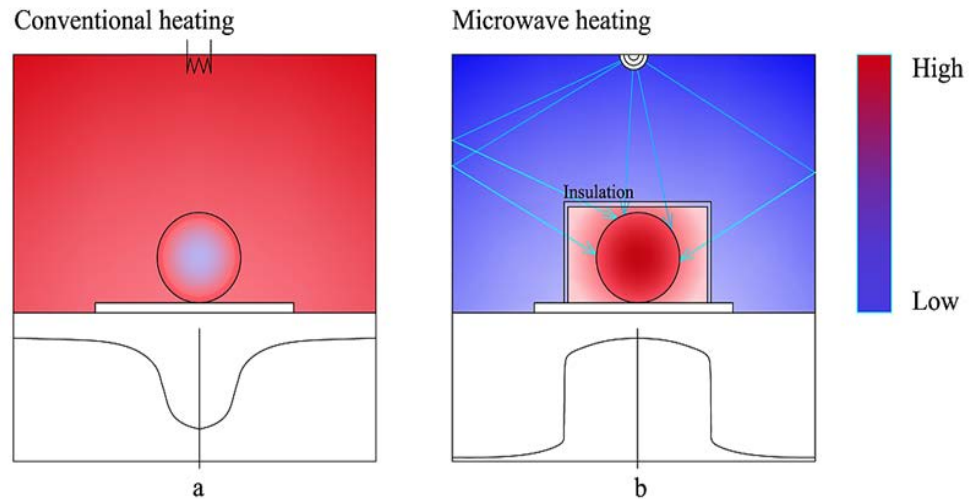


Figure 1.3: Conceptual illustration of heating gradient and temperature profile of a material in (a) conventional and (b) MW heating adapted from (Fernández et al., 2011)

Today, the use of MW is well established in domestic applications. The industrial use of MW spans a vast variety of applications including food processing, sterilization and pasteurization, drying processes, vulcanization of rubber and plastic compounds, polymerization or curing of polymers and resins as well as thermal treatment of ceramics (Menéndez et al., 2010). Recently, MW technology is being explored for pre-treatment of biomass (Li et al., 2016). However, this emerging technology is yet underutilized in biomass gasification technologies and has a great potential for thermal tar removal applications especially on a large scale.

## 1.5 Problem statement

Operation of SOFC coupled with gasifier at appropriately low S/C ratios is a definite challenge. It requires extensive removal of contaminants especially tar from PG which is considered a barrier to successful use of BIG–SOFC systems (Pumiglia et al., 2017). Also, maintaining SOFC operating temperature of 700–900 °C is an energy intensive requirement which has always been done by an external source i.e. electric furnace. Tar thermal cracking offers advantages of significant tar conversion along with increasing the PG heating value and the heat generated for tar thermal cracking can be utilized as a heat source for SOFC. Nevertheless, investigated conventional tar thermal cracking systems so far are on lab scale as well as based on inefficient method of transferring energy i.e. electrical furnaces. The drawbacks of electrical furnaces include slow heating, high heat losses, damaging of the reactor walls and limiting the tar conversion reactions due to heat transfer mechanism from the external of the reactor in which heat transfer occurs from surface to the core of the material. Consequently, there is a need for technically as well as economically improved scale up tar thermal cracking systems.

MW heating is unique in its capability to overcome the constraints related with conventional heating. With its selective and “volumetric” heating features, MW heating offers the benefit of improved energy transfer efficiency, reduced process heating times and acceleration of the reaction rates. Other benefits include smaller process equipment, better control of the process, equipment availability, cost and maintainability and overall cost effectiveness. MW energy has been exploited in pyrolysis of biomass (Motasemi & Ani, 2012) as well as in pre-treatment and upgrading technologies of biomass (Anis & Zainal, 2014; Kostas et al., 2017).

In this research, a 4.5 kW modified industrial MW system for thermal cracking of tar is developed for its integration with a 10 kW<sub>th</sub> gasifier. The possibility of utilizing the heat generated by MW and carried by PG for generating the operating temperature for SOFC has been investigated. This research has high prospect in providing the evidence that tar thermal cracking using MW heating could be used for commercial small scale (up to 10 kW<sub>th</sub>) gasifiers for an un-interrupted process with the possibility of utilizing heat for additional purposes. It is expected that tar thermal cracking based on MW heating could be taken out from the lab and applied to a commercial small scale BIG–SOFC systems for efficient CHP production.

## **1.6 Objectives of the thesis**

The goal of this research is to setup and evaluate a PG cleaning system mainly based on MW assisted tar thermal cracking which acts as a simultaneous heat source for SOFC operation. Therefore, further objectives of this study are:

- 1) To develop and evaluate the performance of an up–scale MW tar thermal cracking system for PG tar removal from a 10 kW<sub>th</sub> gasifier.
- 2) To develop and evaluate an insulated stainless steel chamber to utilize PG sensible heat from MW tar cracking reactor for maintaining SOFC operation temperature.
- 3) To evaluate the performance of SOFC fuelled by cleaned real PG at low S/C ratio under thermal profile maintained by hot PG from MW tar cracking reactor.

## **1.7 Scope of the thesis**

In this project, an experimental setup comprising of complete system from gasifier to electricity using SOFC is established to demonstrate the concept of BIG–

SOFC system. The core of the setup is a temperature controlled MW tar thermal cracking system. A 4.5 kW industrial MW oven with 2.4 GHz frequency was modified to accommodate an  $\text{Al}_2\text{O}_3$  annular reactor inside the MW cavity. Silicon Carbide (SiC) was used as an MW absorber material. The influence of SiC particle size, PG flow rate and MW power were tested in order to obtain optimal conditions in terms of temperature evolution and pressure drop inside the MW reactor. At the optimum conditions, the MW tar cracking reactor was integrated with a throatless air blown type downdraft gasifier after the cyclone separator to investigate tar and particulate removal efficiencies in terms of gravimetric yield. Tar thermal cracking results were used to develop the PG tar reaction kinetic model to determine activation energies and other kinetic parameters.

Then, the potential of using the sensible heat of the hot PG exiting the MW reactor to maintain the SOFC operational temperature inside an insulated SS chamber was evaluated. Afterwards, gas cooling section was added after the SS chamber to remove moisture content before the PG was compressed in a compressor. Further tar reduction via compression was studied at different pressures and a tar condensation mechanism via compression was investigated. Finally, the PG suitability for SOFC in terms of contaminants' removal to their tolerance limits was evaluated after cooling and cleaning system. The remaining contaminant,  $\text{H}_2\text{S}$  was removed using modified coconut shell activated carbon (CSAC) before the SOFC performance on cleaned PG was examined. Short term and long term test campaigns on planar single SOFC on open circuit and under load conditions were conducted to evaluate cell's performance on cleaned PG with appropriately low S/C ratio inside a SS chamber. Post investigations using Scanning Electron Microscopy (SEM) was

done to identify any contamination and changes in the microstructure of the anode of SOFC using PG.

## **1.8 Outline of the thesis**

The thesis is divided into five chapters:

Chapter 1 gives an introduction on BIG-SOFC systems as an efficient decentralized CHP production option as well as problems related with PG contaminants especially tar. Tar content and overview of tar thermal cracking are briefly presented together with MW heating as an alternative method for tar thermal cracking. Also included are the problem statement, objectives and solution of problems.

Chapter 2 presents literature review of biomass gasification in downdraft gasifier, tar classification and its removal via thermal cracking. Theory related to kinetics of tar thermal cracking, MW energy and SOFC are also presented. This chapter critically reviews the vast literature regarding (i) the influence of various PG contaminants on SOFC anodes to conclude their probable tolerance limits for safe SOFC operation and (ii) the cleaning methods for these contaminants to choose best cleaning option with the techno-economic point of view.

Chapter 3 provides details on the experimental set up including downdraft gasifier, MW tar cracking system, PG cooling and cleaning system and the SOFC testing system. The details of materials and methods used to carry out experiments together with equipment and techniques used for sampling and analysis of PG composition, tar, particulates, HCl and H<sub>2</sub>S are also presented.

Chapter 4 presents experimental results and corresponding discussions on them and is divided into seven sections: (1) biomass materials' characterization, (2) gasifier characterization (3) thermal heating characteristics of MW reactor and its integration with the gasifier (4) thermal cracking of tar from PG and global reaction kinetic model of PG tar, (5) evaluation of cooling and (6) cleaning system for other PG contaminants' removal and lastly (7) performance evaluation of SOFC on cleaned PG with and without electrical load. In general, tar thermal cracking results from current scale up system are compared to previous lab scale study by Anis and Zainal (2014) and Anis et al. (2013). SOFC performance in this work is also compared with other studies on SOFC operation on PG.

Chapter 5 summarizes the findings and gives conclusions of the present study. Based on these results, recommendations for further research in this area are proposed.



## CHAPTER TWO

### LITERATURE REVIEW

#### 2.1 Biomass materials

Biomass is non-fossilized and biodegradable organic material from plant, animal and micro-organisms mainly characterized into four main types, woody plants, herbaceous plants, aquatic plants and manures (McKendry, 2002a). Woody biomass and herbaceous biomass with low moisture content (<40 wt%) are considered most suitable for thermochemical conversion of biomass (McKendry, 2002b). Fuel analysis in terms of gross components such as volatile matter (VM), moisture content, ash and fixed carbon (FC) is known as proximate analysis of a fuel. It is used to establish the first measure of the suitability of biomass material for gasification. VM and FC contents of biomass fuels are found to be higher than bituminous coal indicating easiness of fuel ignition. The ash fraction is mostly less in woody biomass as compared to husk and straw materials. The HHV of biomass fuels normally ranges from 17 to 21 MJ kg<sup>-1</sup>. The ultimate analysis presents the elemental composition of the fuel. It is required to determine the theoretical air/fuel ratio in various gasification processes and in evaluating the potential emissions. The proximate and ultimate analysis of different biomass materials and coal are given in Table 2.1 for comparison.

For biomass gasification integrated with SOFC systems, the selected biomass feedstock must have appropriate physical and chemical properties. Amongst the physical properties, low moisture content and high bulk density are desirable. Thermal efficiency of the gasification reduces if the moisture content is more than 40

wt% (Hosseini et al., 2012) due to the energy used for biomass drying inside the gasifier. This also reduces the reaction temperature which results in PG with higher tar levels and low LHV (Kirnbauer et al., 2013). The density affects the feeding to the gasifier. As far as chemical properties are concerned, biomass fuels with high calorific value and low ash, chlorine and sulfur contents are preferred. Where high ash content can cause agglomeration, erosion and corrosion problems, the high sulfur and chlorine contents can end up as high H<sub>2</sub>S and HCl concentrations in the PG which needs to be removed before its utilization in SOFC (see Section 2.6.4 and 2.6.5). Table 2.1 compares some biomass feedstocks with bituminous coal.

Table 2.1: Ultimate and proximate analysis of some biomass materials compared with bituminous coal (McKendry, 2002a; Zabaniotou, 2014)

Biomass type	Ultimate analysis (% w/w, dry basis)					Proximate analysis (% w/w)				LHV (MJ/kg)
	C	H	O	N	S	Ash	VM	FC	M	
Larch wood	44.15	6.38	49.32	0.12	-	0.12	76.86	14.86	8.16	19.45
Camphor wood	43.43	4.84	38.53	0.32	0.1	0.49	72.047	14.75	12.29	17.48
Wood sawdust <sup>1</sup>	46.2	5.1	35.4	1.5	0.06	1.3	70.4	17.9	10.4	18.81
Rice husk	45.8	6.0	47.9	0.3	-	0.8	73.8	13.1	12.3	13.36
Rice straw	38.61	4.28	37.16	1.08	0.65	12.64	65.23	16.55	5.58	14.40
Wheat straw	46.1	5.6	41.7	0.5	0.08	6.1	75.8	18.1	(dry basis)	17.2
Switch grass	47	5.3	41.4	0.5	0.1	4.6	58.4	17.1	20	18.7
Cotton stem	42.8	5.3	38.5	1.0	0.2	4.3	72.3	15.5	7.9	15.2
Bituminous coal	80.9	6.1	9.6	1.55	1.88	9	35	45	11	34

<sup>1</sup> derived from tropical wood

## 2.2 Biomass gasification

In thermo chemical process of gasification, the biomass is converted into a gaseous mixture through partial oxidation in a gasifier. This gas mixture referred to as PG consists of hydrogen, carbon monoxide, methane and carbon dioxide along

with nitrogen, water vapour and impurities. Gasification inside a gasifier involves four processes; drying, pyrolysis, oxidation and reduction summarized in Table 2.2.

Table 2.2: Overview of biomass gasification processes

Sub-process/ Temp (°C)	Processes involved/ Reaction equations – Reaction name	Products in PG at sub-process
Drying < 200	Drying of biomass	
Pyrolysis 200-600	Release of VM (gas, vaporized tar, char)	CO, H <sub>2</sub> , H <sub>2</sub> O, CO <sub>2</sub> , CH <sub>4</sub> , C <sub>2</sub> H <sub>2</sub> , N <sub>2</sub> , tar
Reduction 600-1000	C + CO <sub>2</sub> ↔ 2CO ( $\Delta H_{298}^0 = +172$ kJ/mol) – Boudouard C + H <sub>2</sub> O ↔ CO + H <sub>2</sub> ( $\Delta H_{298}^0 = +131$ kJ/mol) – Water-gas C + 2H <sub>2</sub> ↔ CH <sub>4</sub> ( $\Delta H_{298}^0 = -75$ kJ/mol) – Methanation CO + H <sub>2</sub> O ↔ CO <sub>2</sub> + H <sub>2</sub> ( $\Delta H_{298}^0 = -41$ kJ/mol) – Water-gas shift CH <sub>4</sub> + H <sub>2</sub> O ↔ CO + 3H <sub>2</sub> ( $\Delta H_{298}^0 = +206$ kJ/mol) – Steam-methane reforming	CO, H <sub>2</sub> , H <sub>2</sub> O, CO <sub>2</sub> , CH <sub>4</sub> , C <sub>2</sub> H <sub>2</sub> , N <sub>2</sub> , tars, particles, H <sub>2</sub> S, NH <sub>3</sub>
Oxidation 1000-1500	C + 0.5O <sub>2</sub> ↔ CO ( $\Delta H_{298}^0 = -111$ kJ/mol) – Char partial combustion C + O <sub>2</sub> ↔ CO <sub>2</sub> ( $\Delta H_{298}^0 = -399$ kJ/mol) – Char total combustion H <sub>2</sub> + 0.5O <sub>2</sub> ↔ H <sub>2</sub> O ( $\Delta H_{298}^0 = -242$ kJ/mol) – H <sub>2</sub> partial combustion	CO, H <sub>2</sub> , H <sub>2</sub> O, CO <sub>2</sub> , CH <sub>4</sub> , C <sub>2</sub> H <sub>2</sub> , N <sub>2</sub> , tars, particles, H <sub>2</sub> S, NH <sub>3</sub>

In successive steps, biomass is dried, then pyrolysed into gases and char which react further with gasifying agent hence producing PG. The required energy for gasification is provided by partial combustion of biomass through exothermic reactions (see Table 2.2) within the same gasifier. Alternatively, the heat could be supplied indirectly outside of the gasifier to raise the gasification temperature. The composition of PG and impurities depend on the type of feedstock used, gasifier type, the gasification agent and gasifier operating parameters. The six impurities present in PG are particulates, tar, traces of sulfur, chlorine, nitrogen and alkali compounds may exist in different phases of appearances as shown in Figure 2.1 and are comprehensively overviewed in Table 2.3.

Table 2.3: Overview of impurities in producer gas (Asadullah, 2014; Woolcock & Brown, 2013)

Impurity	Source/ Description of impurity	Effects of impurity	Gas quality requirements (Asadullah, 2014)
Particulate matter	<ul style="list-style-type: none"> <li>- Solid agglomerations of unreacted carbon and ash (K, Na, Ca, SiO<sub>2</sub>, Fe, Mg)</li> <li>- Also, condensed tar and alkali species</li> <li>- Elutriated bed material/ catalysts from FB gasifiers</li> <li>- Size range from &lt; 1 µm to 100 µm</li> </ul>	<ul style="list-style-type: none"> <li>- Fouling on reactor walls and bed materials</li> <li>- Clogging of gas cleaning filters</li> <li>- Blocking engine nozzles and ICE systems</li> <li>- Corrosion and erosion of downstream equipment and turbine blades</li> </ul>	ICE: < 50 (PM10) Turbine: < 20 (PM0.1) (unit: mg Nm <sup>-3</sup> ) (PM10 = 10 µm and PM0.1 = 0.1 µm)
Tar	<ul style="list-style-type: none"> <li>- Formed during pyrolysis and reactions with char</li> <li>- Complex mixture of diverse organic (aromatic) compounds</li> <li>- All hydrocarbons with molecular weights &gt; benzene are called Tar</li> <li>- In vapour phase inside gasifier</li> </ul>	<ul style="list-style-type: none"> <li>- Condenses from 300 °C below and becomes sticky</li> <li>- Plugging and fouling of pipes, tubes, equipment</li> <li>- Clogging of gas cleaning filters</li> <li>- Abrasion of turbine blades</li> <li>- Deactivate catalysts/ sorbents for reforming/cleaning</li> <li>- Contaminate water of wet clean-up processes</li> </ul>	Compressors: < 500 ICE: < 100 Turbine: < 5 (all vapour) (unit: mg Nm <sup>-3</sup> )
Sulfur compounds: Mainly H <sub>2</sub> S	<ul style="list-style-type: none"> <li>- Biomass inherent 0.1% wt Sulfur lower than Coal (1% wt)</li> <li>- H<sub>2</sub>S in PG varies 20 ppm – 200 ppm</li> <li>- Stringent cleanup not required for most of the applications except SOFC (see Section 2.6.4)</li> </ul>	<ul style="list-style-type: none"> <li>- Poison catalysts for upgrading PG and catalysts for gas cleanup</li> <li>- Sulphur compounds corrode metal surfaces</li> </ul>	ICE: - Turbine: < 1 (unit: ppm)
Halides: Mainly HCl	<ul style="list-style-type: none"> <li>- Chlorine in biomass vaporizes in gasifier and react with water vapour to form HCl vapour (boiling point 57 °C)</li> <li>- HCl in syngas varies 99 ppm to 200 ppm</li> <li>- HCl (vapours with other contaminants) form NH<sub>4</sub>Cl, NaCl</li> </ul>	<ul style="list-style-type: none"> <li>- Hot corrosion of turbine blades</li> <li>- Condensed NH<sub>4</sub>Cl and NaCl causes fouling and they deposit in cooler downstream piping and equipment</li> </ul>	ICE: - Turbine: < 0.5 (unit: ppm)
Alkali compounds mainly K, Na	<ul style="list-style-type: none"> <li>- Biomass contains alkali and alkali earth metals</li> <li>- Alkali based catalysts and transition metal promoters also contribute alkali metal contaminants</li> <li>- Vaporize above 600 °C leaving reactor as aerosols and/or vapours and can readily condense downstream</li> </ul>	<ul style="list-style-type: none"> <li>- condensed form causes fouling and corrosion in downstream applications</li> <li>- Agglomeration of the bed materials</li> <li>- Promotes slagging of ash in equipment</li> <li>- Poison some catalysts and damage ceramic filters</li> </ul>	ICE: - Turbine: < 50 (unit: ppb)
Nitrogenous species: mainly NH <sub>3</sub> , HCN	<ul style="list-style-type: none"> <li>- Originate from the nitrogen content and protein containing materials in biomass</li> <li>- Predominantly NH<sub>3</sub> is the primary contaminant</li> <li>- Typically in gaseous phase (boiling point &lt;30 °C)</li> </ul>	<ul style="list-style-type: none"> <li>- Not sensitive to engines and turbines</li> <li>- To be controlled to check NOx emissions</li> <li>- Poison some catalysts</li> </ul>	ICE: - Turbine: -

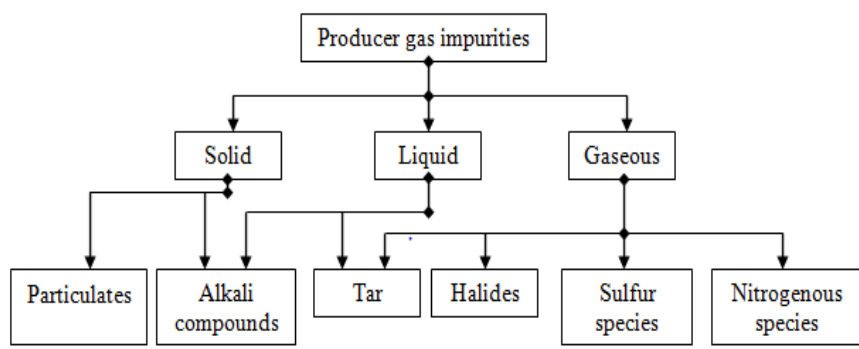


Figure 2.1: Overview of impurities in biomass gasification gas (Nagel, 2008)

The available gasifier systems for biomass gasification are categorized as fixed bed and fluidized bed gasifiers. Fixed bed gasifiers are further divided into updraft and downdraft gasifiers. In updraft (countercurrent) gasifiers (Aljbour & Kawamoto, 2013b), the biomass moves downward from the top while gasifying agent moves upward from the bottom and the PG is collected from the top of the gasifier. As the PG passes through the low temperature pyrolysis and drying zone, it exits with comparatively high tar content, although with lower particulate content due to the filtration on the way up. In downdraft (concurrent) gasifiers (Patra & Sheth, 2015), both biomass and gasifying agent (mostly air) move from the top to the bottom of the gasifier (Figure 2.2). The PG exits at the bottom after passing through the high temperature oxidation and reduction zones, which results in relatively clean gas from tar as compared to updraft gasifiers.

In fluidized bed gasifiers, the biomass fuel and bed material (sand/catalyst) are fluidized with the help of excessive air/gas (Loha et al., 2014). These types of gasifiers operate at uniform but lower temperature (<900 °C) to avoid ash melting. But tar and particulate load in PG is high in fluidized bed gasifiers as compared to downdraft gasifiers. Characteristics of commonly used gasifiers are compared in Table 2.4.

Table 2.4 : Comparison of commonly used biomass gasifiers (Knoef, 2005; Ruiz et al., 2013)

	Downdraft	Updraft	Fluidized bed	Circulating fluidized bed	Dual Fluidized bed
Gasification agent	Air	Air	Air/ H <sub>2</sub> O/ O <sub>2</sub>	Air/ H <sub>2</sub> O/ O <sub>2</sub>	H <sub>2</sub> O
PG temperature (°C)	700	200–400	800–1000	-	800–1000
Reaction temperature (°C)	~ 1090	-	800–1000	-	800–1000
PG LHV (MJ N m <sup>-3</sup> )	4.5–5.5	5.5	3.7–8.4	4.5–13	14–18
Tar in PG (g Nm <sup>-3</sup> )	0.01–5	30–150	3.7–62	4–20	0.2–2
Particles in PG (g Nm <sup>-3</sup> )	0.02–8	0.1–3	20–100	8–100	8–100
Ash in syngas	Low	High	High	High	High
Reactor Size (MW <sub>th</sub> )	<1	0.1–20	1–50	20–200	-
Hot gas efficiency (%)	85–90	90–95	89	89	90–95
Technology	Proven, simple with low investment cost		Proven with coal, complex with high investment cost		

### 2.2.1 Downdraft gasifier

As far as the selection of the gasifier for BIG–SOFC systems is concerned, downdraft gasifier seems to be a good selection for typical SOFC power generation modules already in demonstrative operation in the ranges between 25–250 kW (Ramadhani et al., 2017). Also, downdraft gasifier has moderate cost and most importantly produces relatively low level of tar as compared to other gasifiers as shown in Table 2.4. For the SOFC based power generation systems around 1 MW range, fluidized bed gasifier might be a good option but such gasifiers produce higher level of impurities and more energy and cost would be required to clean the higher amounts of impurities. Salient features of downdraft gasifier used in this work are discussed in this section below.

Downdraft gasifiers are basically categorized into two types: throated and throatless gasifiers as visualized in Figure 2.2. In throated gasifiers, gases and biomass flow concurrent through a descending packed bed supported across a constriction or a throat. Temperature at the throat or the combustion zone is around

900–1200 °C and uniformly distributed over the cross-section and allows most of the tar contained in the pyrolysis products to be cracked.

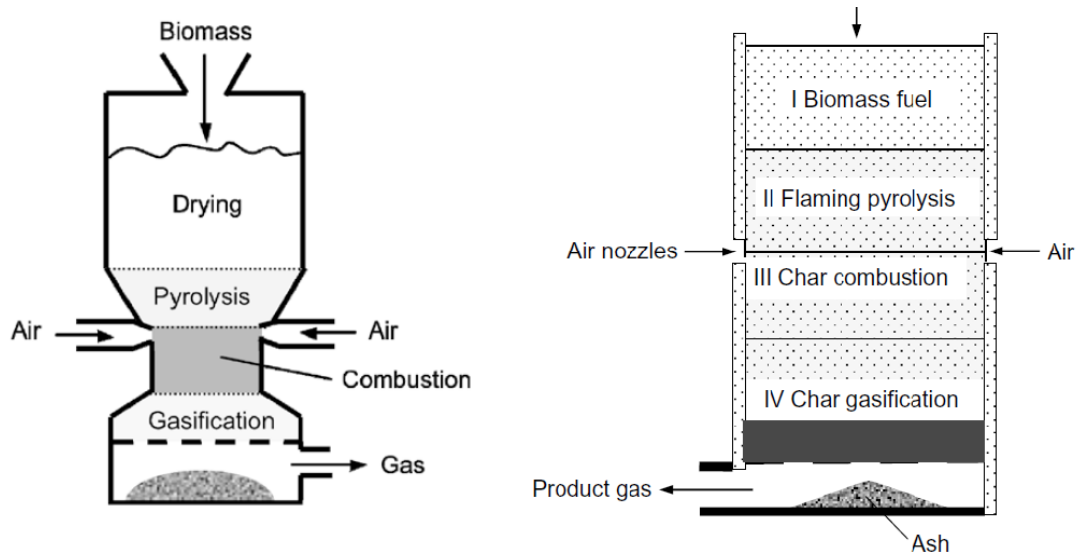


Figure 2.2: Sequential steps of gasification in throated (left) and throatless (right) fixed bed downdraft gasifier (Basu, 2010)

The throatless gasifier consists of a cylindrical vessel without a throat in which the hearth is located at the bottom. The uniform passage of air and biomass down the gasifier keeps high local temperatures to be constant. Gas passes through a long and uniformly high temperature char bed where the pyrolysis components are cracked. A throatless design allows unrestricted movement of the biomass down the gasifier that avoids bridging or channelling, which might occur in the throated type.

### 2.2.1(a) Gasifier performance

Gasifier performance is usually presented by the quantity and more importantly the quality of PG generated. In general, cold gas efficiency and heating value of PG are the important parameters in determining the performance of a gasifier. Cold gas efficiency ( $\eta_{cg}$ ) can be defined as the energy content of the producer gas in comparison to that of biomass fuel as expressed below:

$$\eta_{cg} = \frac{LHV_{PG}Q_{PG}}{LHV_b\dot{m}_b} \times 100 \quad 2.1$$

where:

$LHV_{PG}$  = lower heating value of the producer gas ( $\text{MJ Nm}^{-3}$ )

$Q_{PG}$  = volumetric flow rate of the producer gas ( $\text{Nm}^3 \text{h}^{-1}$ )

$LHV_b$  = lower heating value of the biomass fuel ( $\text{MJ kg}^{-1}$ )

$\dot{m}_b$  = mass flow rate of the biomass fuel ( $\text{kg h}^{-1}$ )

Based on the PG composition,  $LHV_{PG}$  can be calculated and is dependent on the percentage volume fraction of  $\text{H}_2$ ,  $\text{CO}$  and  $\text{CH}_4$  as follow:

$$LHV_{PG} = x_{\text{H}_2}LHV_{\text{H}_2} + x_{\text{CO}}LHV_{\text{CO}} + x_{\text{CH}_4}LHV_{\text{CH}_4} \quad 2.2$$

where  $x$  is the volume fraction of each gas and the LHV of each gas is 10.757, 12.641 and 35.787  $\text{MJ Nm}^{-3}$  for  $\text{H}_2$ ,  $\text{CO}$  and  $\text{CH}_4$ , respectively (Waldheim & Nilsson, 2001).

### 2.2.1(b) Effects of operating parameters on gasification process

In addition to the biomass type and gasifier used, the gasification agent and gasifier operating parameters especially equivalence ratio (ER) also influence the composition of PG. Air is the most common and economical gasification agent used which yields low heating value gas of 4–6  $\text{MJ Nm}^{-3}$  (McKendry, 2002b) for all gasifiers as seen in Table 2.4. Steam gasification in fluidized bed gasifiers produces 10–16  $\text{MJ Nm}^{-3}$  (Bridgwater, 2003) while dual fluidized bed gasifiers produce gas as high as 12–18  $\text{MJ Nm}^{-3}$  (LHV) (Göransson et al., 2011).

ER is defined as the ratio between the air-fuel ratio of gasification process to stoichiometric air-fuel ratio and represented mathematically as:



$$ER = \frac{\text{Air flow rate} / \text{Biomass consumption rate}}{|\text{Air flow rate} / \text{Biomass consumption rate}|_{\text{stoichiometric}}} \quad 2.3$$

The stoichiometric ratio of air flow rate to biomass consumption rate is 5.22 m<sup>3</sup> air/kg of wood (Zainal et al., 2002).

ER is a key parameter because it influences the heating value of PG significantly. Higher ER value reduces the percentages of H<sub>2</sub> and CO hence resulting in low heating value PG due to the greater oxidation environment in the gasifier. On the other hand, lower ER results in higher heating value gas but yield considerably high levels of tar. According to the number of studies, the suitable value of ER is between 0.2 and 0.4 (Gabra et al., 2001; Zainal et al., 2002) to get better heating value and controlled tar level.

### 2.2.2 Tar formation, composition and classification

Biomass gasification is a complex process in which biomass is sequentially dried and pyrolysed to form gases and char at low temperatures of 200–500 °C. Tar formation starts in the biomass and continues externally as depicted in Figure 2.3.

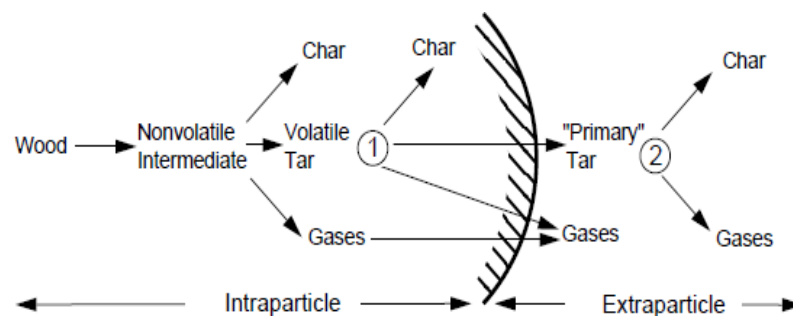


Figure 2.3: Formation and conversion of tar (Morf, 2001)

Pyrolysis reaction forms the primary char, volatile tars and gases. Primary tars are the inevitable products when carbonaceous fuel is pyrolysed. Cellulose,

hemicellulose and lignin components of biomass break down into primary tar that contains oxygenates and primary organic condensable molecules. Secondary tar having heavier molecules is the result of polymerization reactions when the primary tar undergoes further reactions at the temperature above 500 °C. Further temperature increase results in destroying of primary tar products and forming of tertiary products. This tar evolution as a function of temperature is shown in Figure 2.4.

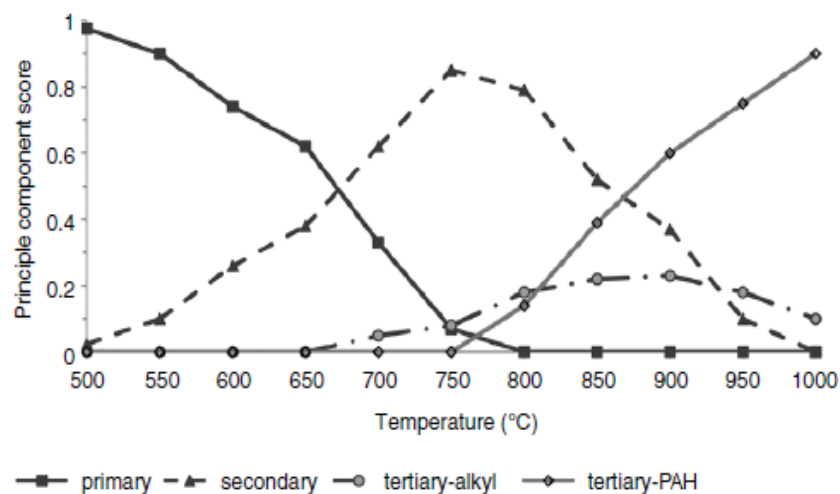


Figure 2.4: Tar evolution as a function of temperature (Milne et al., 1998)

### 2.2.2(a) Tar definition

A number of definitions of tar are discussed in the literature and depends on the methods for sampling and analysis of tar and its tolerance limits for a particular end user application. Milne et al. defines tar as the organics, generally largely aromatic which are produced under gasification of any organic material (Milne et al., 1998). However, the non-condensable products such as benzene and ethylene are also of the concerned tar for fuel cell applications. Tar is also defined as a complex mixture of condensable hydrocarbons, comprise of single to multiple ring aromatic compounds along with other oxygen containing hydrocarbons and complex

Polycyclic Aromatic Hydrocarbons (PAH) (Devi et al., 2005). Agreed upon definition is that all hydrocarbons with molecular weight higher than benzene are Tar (Maniatis & Beenackers, 2000).

### **2.2.2(b) Tar composition and classification**

One approach to classify tar is based on their reactivity to compare products from various gasifiers used. In this classification, tar compounds are divided into four classes as primary products (cellulose-, hemicellulose- and lignin- derived), secondary products (phenolic and olefins), alkyl tertiary products (methyl derivatives of aromatics) and condensed tertiary products (PAH series) (Milne et al., 1998). Tertiary products appear only after the primary products are destroyed (Figure 2.4). The lists of tar components present in the PG from various gasifiers are tabulated in Table 2.5. Tar compounds produced from downdraft gasifiers are mainly composed of light aromatic and light poly-aromatic hydrocarbons that are classified into class 3 and 4 tar, respectively. On the other hand, updraft gasifiers mainly produced heavy oxygenated-based tar compounds and heterocyclic compounds that are class 1 and 2 tar, respectively.

Fundamentally tar related problems are not only related to the quantity, but also the composition and properties of the tar that are associated with tar condensation behaviour which is an integral effect of all the tar components present in PG. According to the Raoult's Law, when the partial pressure of tar vapour in PG is higher than the saturation pressure of tar, the gas becomes oversaturated (Reid et al., 1987) and the condensation of the saturated vapor occurs.